J Mater Sci (2007) 42:6093–6101
DOI 10.1007/s10853-006-1155-8

Enthalpy relaxation of reactive graphitic nanofibers reinforced epoxy

Amin Salehi-Khojin · Soumen Jana · Wei-Hong Katie Zhong

Received: 10 January 2006 / Accepted: 17 October 2006 / Published online: 16 April 2007
© Springer Science+Business Media, LLC 2007

Abstract The enthalpy relaxation of an epoxy resin modified by three different concentrations of reactive-Graphitic Nanofibers (r-GNFs) has been investigated by standard and modulated differential scanning calorimetry (DSC). From DSC scan at 10 °C/min following cooling at various rates through the transition region, the apparent activation energy, Δh^*, was evaluated. The non-linearity parameter, χ, was analyzed by the peak shift method for samples annealed at temperature T_g –20 °C for different period of time (up to 167 h). The non-exponentiality parameter, β, was determined based on the inflectional slope of the complex heat capacity. The experimental results showed that the incorporation of r-GNFs into epoxy network causes greater non-linearity, higher apparent activation energy, and broader relaxation time distribution than the neat epoxy resin. These values were optimum for epoxy resin with 0.3 wt% of r-GNFs.

Introduction

Epoxy resins are a class of important thermosetting polymers, which are widely used as high performance adhesives, matrices of composite materials and electronic encapsulating materials [1, 2]. In many of these applications, thermal and dimensional stability of epoxy resin are very important, and can affect the service life and overall performance of polymeric systems. For this reason, recent research efforts on epoxy resins have been focused on improving their thermal stability, improving glass transition temperature, and increasing dimensional stability [3, 4].

In this respect, compared to the bulk polymers, nano-scale additives-filled polymers have been shown to have improved thermal, mechanical and physico-chemical properties [5–7]. These properties depend on the properties of the individual components (polymer matrix and filler) and the degree of interaction between the polymer chains and the surface of the nano-scale fillers. The strong interface between nano-fillers and polymeric materials leads to better comprehensive performance and dimensional stability of the nano-composites. GNFs are attractive additives that can be applied to achieve this goal. Each GNF atomic structure presents a unique, reactive surface and atomic spatial arrangement to an external polymer matrix, thus permitting a wide range of options for promoting GNFs/polymer covalent bonding. The structure of GNFs can be controlled through the catalyst and thermal conditions in their production. The individual graphene planes compromising the carbon nanofiber are oriented either parallel, perpendicular, or in a herringbone pattern relative to the long axis of a GNF (Fig. 1) [8]. In this research work, we used herringbone GNFs with functionalized group of 3,4′-oxydianiline (ODA) as shown in Fig. 2. Along the nanofibers, the graphene plate edges are exposed and offer potential for the attachment of reactive groups. Through our study, we have the reactive groups react with the oxirane group of butyl glycidyl ether (BGE) diluent, and consequently, the super molecule, r-GNF–ODA, was formed (Fig. 3 [9]). Because of existence of –OH– with reactive –H attached, it can involve the curing reaction of the epoxy resin, and then incorporate nanofibers into cured epoxy structures. This r-GNFs/epoxy is a unified epoxy resin system, which is a real nano-epoxy matrix instead of a simple mixture or a nano-composite.

A. Salehi-Khojin · S. Jana · W.-H. Katie Zhong (✉)
Department of Mechanical Engineering and Applied Mechanics, North Dakota State University, Fargo, ND 58105, USA
e-mail: Katie.Zhong@ndsu.edu

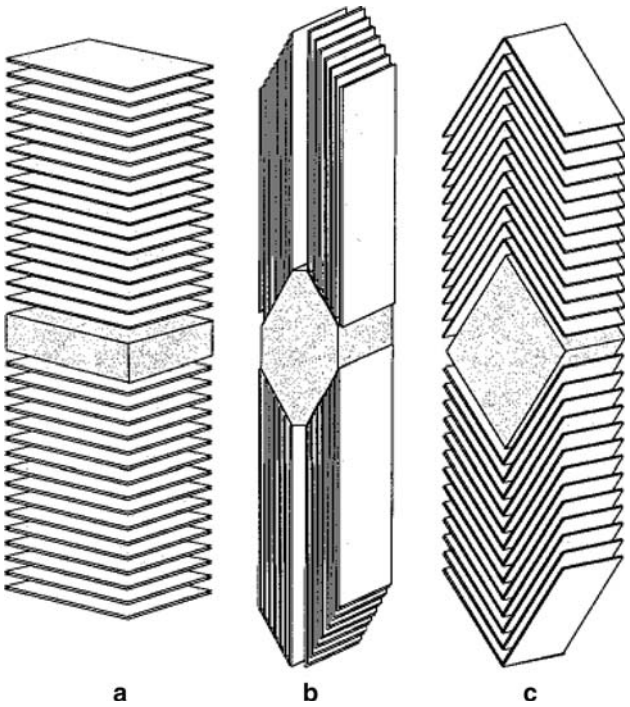

Fig. 1 Schematic representation of the platelet (**a**), ribbon (**b**), and herringbone (**c**) structured GNF synthesized from metal catalyst particles [8]

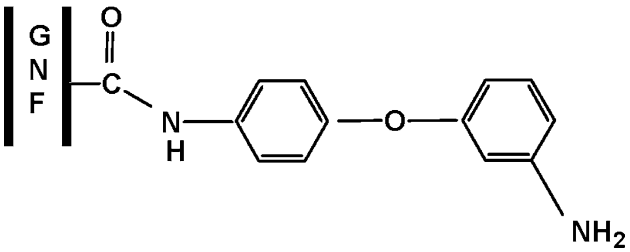

Fig. 2 Chemical structure of GNF-ODA nanofiber

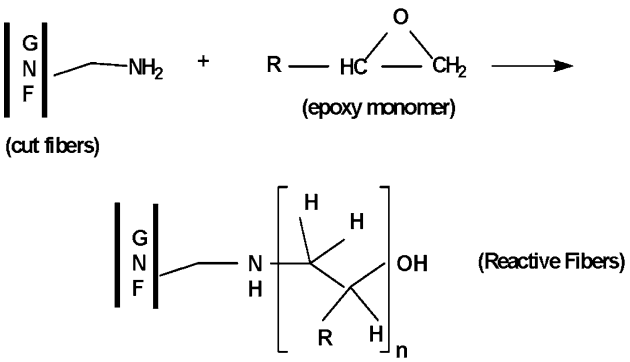

Fig. 3 Formation of reactive GNF [9]

In our laboratory, we have developed a series of nano-epoxy materials, which can be applied as matrices for structural composite. We have studied the mechanical and thermal properties of these nano-epoxy materials. Significant improvements in these properties have been achieved even at low concentrations of r-GNFs (<0.5 wt%) in the nano-epoxy matrix. For example, enhancements of ca. 26% in strength, 30% in modulus and 14 °C in T_g have been obtained in a nano-epoxy with 0.3 wt% of r-GNFs (this work will be reported elsewhere). This material was developed to improve the interfacial property between ultra high molecular weight polyethylene (UHMWPE) fiber and epoxy matrix for NASA Space Radiation Shielding Program. Thus, we also have studied the wetting and adhesion properties of the nano-epoxy matrix materials with UHMWPE fibers. The results showed significant improvement in these properties when the concentration of the r-GNFs is as low as 0.3 wt%. It appears that there is an optimum combination of compositions in the nano-epoxy, which is relevant to the molecular structures of the resulting epoxy network attributed to these advanced overall performances. The network characteristics of a thermoset resin also impact the thermal and dimensional stabilities of the material system. In addition, it has been predicted that during its service life that this nano-epoxy matrix would be exposed to an environment that can cause physical aging. Therefore, a study of thermal and dimensional stabilities of this matrix system is critically significant.

It is known that dimensional stability of a polymeric material is closely related to relaxation phenomena that occur in the glassy state [3, 4]. For this reason, in this study, these phenomena were investigated for nano-epoxy matrix with different concentrations of r-GNFs (up to 0.5 wt%) by standard and modulated differential scanning calorimetry (DSC). Fully cured samples were annealed at a temperature of T_g –20 °C for the length of time selected (up to 167 h), and the enthalpy relaxation was analyzed by the peak shift method [10]. From DSC scan at 10 °C/min following cooling at various rates through the transition region, the apparent activation energy and non-exponentiality parameter were evaluated.

Theory

When a polymer is cooled from rubbery state through glass-transition region to the glassy state, the polymer changes from an equilibrium state (above T_g) into a non-equilibrium state (below T_g). The decrease of volume (V), enthalpy (H), and entropy (S) can follow the decease in temperature during cooling, which reveals the polymer is in equilibrium. Through the glass-transition region, the decrease in V, H and S cannot follow the decrease in temperature (Fig. 4 [11]). This behavior of a polymer can be explained by the change in the mobility of macromolecular

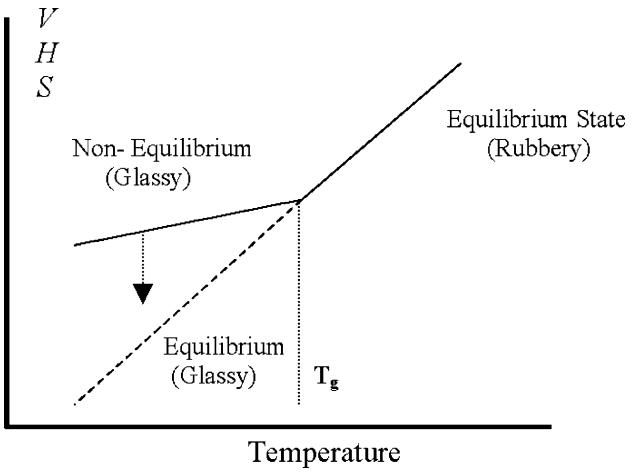

Fig. 4 Schematic illustration of the dependence of volume V, enthalpy H and entropy S as a function of temperature [11]

segments when it goes from rubbery state into glassy state: when $T > T_g$, the mobility of the molecular segments is great; when $T < T_g$, the mobility of macromolecular segments is substantially reduced. The non-equilibrium state is unstable and the polymer searches for an equilibrium structure. This approach of the structure towards equilibrium is usually called structural relaxation [11].

The kinetics of structural relaxation depends on both non-linearity and non-exponentiality parameters. To describe the effect of non-linearity on the relaxation structure, the Tool–Narayanaswamy–Moynihan equation, which illustrates dependence of relaxation time on both the temperature and the structure, is widely used [12–14]. The equation is written as follows:

$$\tau = \tau_0 \exp\{[(\chi \Delta h*)/(RT)] + [(1-\chi)\Delta h*/(RT_f)]\} \quad (1)$$

where τ_0 is a reference relaxation time, Δh^* the apparent activation energy of enthalpy relaxation, T_f the fictive temperature identifying the dependence of relaxation time to the structure of the glass, R the universal constant and χ is the non-linearity parameter which determine the relative contributions of temperature and structure to relaxation time [15]. The non-linearity parameter is a material constant, independent of annealing temperature, annealing time and heating rate.

On the other hand, the Kohlrausch–Williams–Watt equation can be used for relating distribution of relaxation time to non-exponentiality parameter. This equation is usually described by Williams and Watts [16]:

$$\phi(t) = \exp[-(t/\tau)^{\beta}] \quad (2)$$

where β is the non-exponentiality parameter, and is inversely related to the width of relaxation time distribution.

The parameters, Δh^*, χ and β in the above equations describe the response of polymeric materials to any thermal history, and can be used to characterize the effect of nanofibers on the segmental mobility of epoxy networks.

Experiments

Materials and preparation of nano-epoxy matrices

The epoxy resin used in this study was Epon 828 and the curing agent was EPIKURE^{TM} W purchased from Miller-Stephenson Co.. The functionalized graphitic nanofibers, GNF–ODA, were provided by Vanderbilt University and the reactive diluent, butyl glycidyl ether (BGE) from Lancaster Synthesis Inc., was purchased through VWR.

The nano-fibers, GNF–ODA, were carefully weighed and placed in a pear shaped boiling flask. Then the reactive diluent was weighed and added to the flask. The GNF–ODA nanofibers were first mixed with the reactive diluent, BGE, as a dispersant, which has an epoxide group similar to the epoxy. The ratio of the nanofibers to diluent is about 1:50 by weight for the sonication. High-energy sonication was performed with a Branson® S-450D digital sonifier with a 1/8 inch microtip. The disrupter horn of the digital sonifier was immersed in this mixture under different power levels, and the GNF–ODA nanofibers were cut effectively at high power levels. The high-energy sonication was performed at 70 watts. The process was stopped at 180 min elapsed time. Then nanofibers were allowed to react with BGE at a controlled temperature for 36 h. A stable solution containing well-dispersed reactive nanofibers, r-GNFs, (Fig. 3 [9]), were formed. The final mass ratio of r-GNFs to diluent was 1:6 and was controlled by a vacuum oven. This stable solution was added to the blend of epoxy and cure agent, followed by lower-power sonication, thus, nano-epoxy matrices with r-GNFs were prepared. The nano-epoxy matrices with 0.15, 0.3, and 0.5 wt% of r-GNFs were prepared for experiments.

Enthalpy relaxation experiments

For the isothermal annealing experiment, the samples were heated in the DSC (Q1000, TA Instruments Inc.) from room temperature to 200 °C at a constant rate of 10 °C/min and held in this temperature for 20 min in order to erase their previous thermal history. They were then cooled at –20 °C/min to the annealing temperature, which was selected as T_g –20 °C.

After annealing treatment for different periods of time (up to 167 h), the samples were cooled at –20 °C/min to room temperature, and then immediately reheated at 10 °C/min to 200 °C through the glass transition region to obtain

the annealed scan. The same sample was then immediately cooled at –20 °C/min to room temperature, and then immediately reheated up to 200 °C/min at a rate of 10 °C/min, to obtain the reference scan. After these two scans, the same sample was used again for further annealing times.

For the non-isothermal cooling experiment, the samples were heated in the DSC at 10 °C/min from room temperature to 200 °C. After eliminating pervious thermal history, they were cooled at a constant rate of –20 °C/min to room temperature, and then immediately reheated at 10 °C/min to 200 °C, to obtain the reference scan. This cycle was repeated for cooling rates of 20, 10, 5, and 3 °C/min and each time heating scan was recorded. The heating scan obtained after the various cooling rates permit the determination of fictive temperature as a function of cooling rate.

Temperature-modulated DSC (MDSC) was used to measure the complex heat capacity (C_p^*) of all samples. The C_p^* curves for all samples were obtained using an average rate of 1 °C/min, temperature amplitude of 0.5 °C, and modulated period of 60 s.

Results and discussion

Apparent activation energy, Δh^*

Generally the enthalpy loss or enthalpy relaxation (δ_H) corresponds to the area of so-called overshoot on the DSC heating scan. A typical example of overshoot curves for specimens with 0.3 wt% of r-GNFs are shown in Fig. 5. It is obvious that the magnitudes of the peak area are the greatest for the samples that were cooled at the slowest cooling rate (3 °C/min), and the smallest for the samples with cooling rate of 20 °C/min. This means that the extent of aging changes by the cooling rate so that at cooling rate of 3 °C/min, the polymer would gradually approach the equilibrium glassy state with a maximum aging extent while at the cooling rate of 20 °C/min the aging extent is the minimum [17].

This cooling experiment can provide a measure of the apparent activation energy for enthalpy relaxation from the dependence of fictive temperature, T_f, on the cooling rate, q_1. To quantify apparent activation energy, the appropriate equation was proposed by Moynihan et al. [14], which is now widely used:

$$\frac{d\ln|q_1|}{d\left(\frac{1}{T_f}\right)} = -\frac{\Delta h*}{R} \tag{3}$$

where T_f is the fictive temperature (which can be obtained by intersecting the extrapolated glassy enthalpy–temperature line with the liquid enthalpy–temperature line), q_1 is the cooling rate, $R = 8.314$ J mol^{-1} K^{-1}, and Δh^* is the apparent activation energy.

Figure 6 shows a plot of logarithmic cooling rate versus reciprocal of fictive temperature for specimens with different concentrations of r-GNFs (0–0.5 wt%). A near linear relationship was found between ln q_1 and $1/T_f$ for all matrix specimens with different r-GNF concentrations. Based on Eq. (3), the slopes of these straight lines present $\Delta h^*/R$ values. From Fig. 7, Δh^* of all specimens with r-GNFs was increased over pure epoxy, and specimens with 0.3 wt% of r-GNFs showed the highest value. For this concentration, $\Delta h^*/R$ was increased by ca. 60% (from 89 ± 5 kK to 143 ± 8 kK) over pure epoxy specimens.

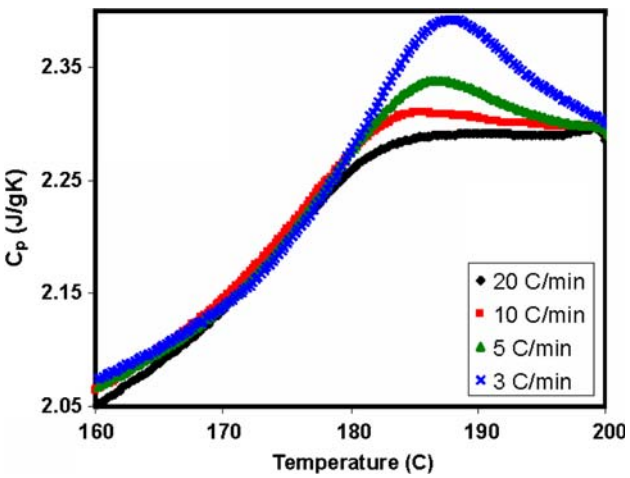

Fig. 5 Typical DSC curves for different cooling rate; the sample is nano-epoxy with 0.3 wt% of r-GNFs

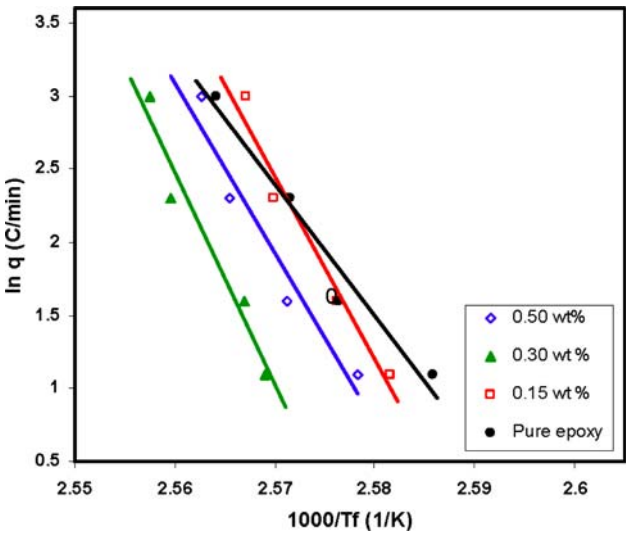

Fig. 6 Logarithmic cooling rate as a function of the reciprocal of fictive temperature

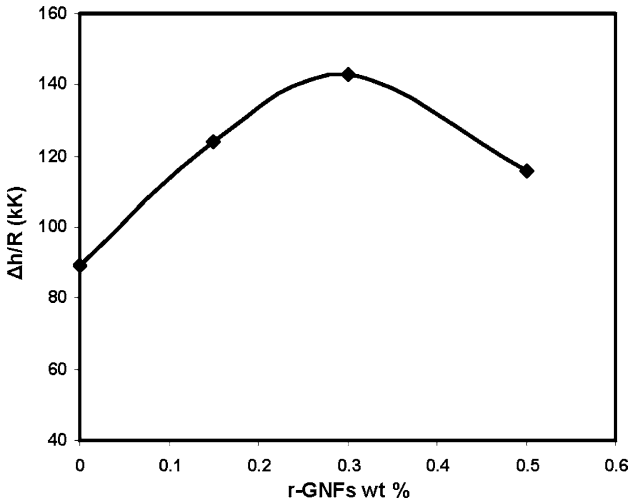

Fig. 7 $\Delta h^*/R$ (kK) as a function of r-GNFs wt%

A reported study on enthalpy relaxation of nano-clay/epoxy nano-composites carried out by Lu and Nutt [18] exhibited an increase in $\Delta h^*/R$ with increasing nano-clay content. It was considered that the increase in Δh^* for the nano-clay/epoxy composites was attributed to restrictive effects of silicate layers. The increase in nano-clay content caused more polymer chain segments to be immobilized on the surface of the silicate layers. A comparison of apparent activation energy, $\Delta h^*/R$, between our results and those given in ref. [18] was made in Table 1. In the study on nano-clay/epoxy with 3, 5, 7 and 9 phr (per hundred resin) of nano-clay, the increase percentage in $\Delta h^*/R$ is ca. 4–9%/phr of nano-clay. However, in our work, the increase percentage is as high as 60–200/wt% of r-GNFs, (or 50–165/phr of r-GNFs). This difference can further indicate that our nano-epoxy system is not a simple mixture of a nano-composite material as revealed in our previous work [19]. We believe that the increase in Δh^* with increasing r-GNF concentrations (up to 0.3 wt%) derives largely from the much stronger restrictive effects of r-GNFs on segmental motion of the epoxy network. In the nano-clay/epoxy nano-composites reported in ref. [18], the nano-clay particles were physically mixed in the epoxy resin, which means there were no chemical bonds between the nano-clay and epoxy resin. Therefore, the restriction caused by the nano-clay layers to the epoxy network is limited to the proximity of the clay surface areas, which led to the slight increase in apparent activation energy, Δh^*. In our nano-epoxy system, the r-GNFs were involved in the epoxy network through the formation of chemical bonding between r-GNFs and epoxy resin, and the r-GNFs can control more areas of epoxy network around the r-GNFs. This leads to larger interphase zone between epoxy network and nanofibers, and stronger nano-epoxy crosslinking structure, as well as more immobilized segments on epoxy network. Thus, more segments of epoxy network, not limited to those near the nanofiber surface area, have to overcome the higher energy barrier to reach the equilibrium state. Thermodynamically, this is reasonable because as the immobilized segments increases, higher energy required reaching epoxy network to activated state, as stated in ref. [18].

It was expected with increasing r-GNFs concentrations in epoxy network, Δh^* would be increased, but this was not the case for 0.5 wt% r-GNFs. This phenomenon can be explained by the higher amount of diluent molecules involved in the epoxy network. Since the r-GNFs are highly polarized and reactive, addition of diluent is necessary to prevent the agglomerating of r-GNFs. In this research work, the saturated solution of r-GNFs in the diluent had a fixed ratio of 1:6; r-GNFs to diluent by weight. For the specimens with 0.15 and 0.3 wt% of r-GNFs, the amount of diluent used in specimens were relatively small (as seen in Table 1: $0.9\% = 0.15\% \times 6$ and $1.8\% = 0.3\% \times 6$, respectively). In this case, the effect caused by the diluent is not obvious, and r-GNFs are the domain that increases the apparent activation energy. When the content of diluent increases further (higher r-GNF wt%), the effect of diluent becomes stronger and leads to a decrease in the crosslink density of epoxy network. It seems this nano-epoxy system is not sensitive to smaller amounts of diluent. Therefore, the apparent activation energy for the sample with 0.5 wt% of r-GNFs was decreased slightly compared to that of the sample with 0.3 wt% of r-GNFs.

Non-linearity parameter, χ

The enthalpy relaxation (annealing) experiments performed over a wide range of annealing time allow the determination of the enthalpy loss, δ_H, on annealing and the value of the peak temperature, T_p, for each aged

Table 1 Comparison of $\Delta h^*/R$ for nano-clay/epoxy [18] and nano-epoxy

Nano-clay/epoxy [18]	$\Delta h^*/R$ (kK)	136	147	165	178	214
	phr[a] of nano-clay	0	3	5	7	9
Nano-epoxy (r-GNFs/epoxy) (this work)	$\Delta h^*/R$ (kK)	89	122	143	120	
	wt% (phr[a]) of r-GNFs	0 (0)	0.15 (0.2)	0.30 (0.4)	0.50 (0.6)	
	wt% (phr[a]) of diluent	0 (0)	0.9 (1.1)	1.8 (2.2)	3.0 (3.7)	

[a] phr is the abbreviation for per hundred resin

nano-epoxy and pure epoxy samples. The δ_H values for all specimens were obtained from the area differences between the annealed DSC curves and unannealed curves of the same samples.

The dependence of the δ_H on the logarithm of the annealing time, t_a, at annealing temperature of T_g –20 °C are shown in Fig. 8. It can be seen that enthalpy losses were increased with time (duration) of relaxation at every relaxation temperature used for isothermal aging. The slopes of δ_H over log (t_a), or $d\delta_H/d\log(t_a)$, for nano-epoxy samples were decreased over pure epoxy samples, and the smallest slope was obtained for nano-epoxy samples with 0.3 wt% of r-GNFs. These results imply that firstly, using nanofiber materials in an epoxy network results in differences in relaxation rates for these materials, and secondly, with 0.3 wt% of r-GNFs in the nano-epoxy, the epoxy network approaches the equilibrium glassy state with the least physical aging extent.

Figure 9 illustrates the endothermic peak temperature, T_p, in DSC curve as a function of annealing time and r-GNFs concentrations. It was found that after annealing, T_p shifts to a higher temperature and increases linearly with the logarithm of the annealing time, t_a. The rate of shift for T_p indicates the restrictive effect of nanofibers in epoxy network. Similar to the trend of enthalpy loss, the specimens with 0.3 wt% of r-GNFs shows the smallest rate for T_p shift, and pure epoxy shows the highest rate. These results imply that the molecular mobility in nano-epoxy matrix with 0.3 wt% of r-GNFs is the minimum.

From the data in Figs. 8 and 9, the non-linearity parameter, χ, can be quantified by the peak-shift method. In this method the dependences of heat capacity to endothermic peak temperature define as follow [20]:

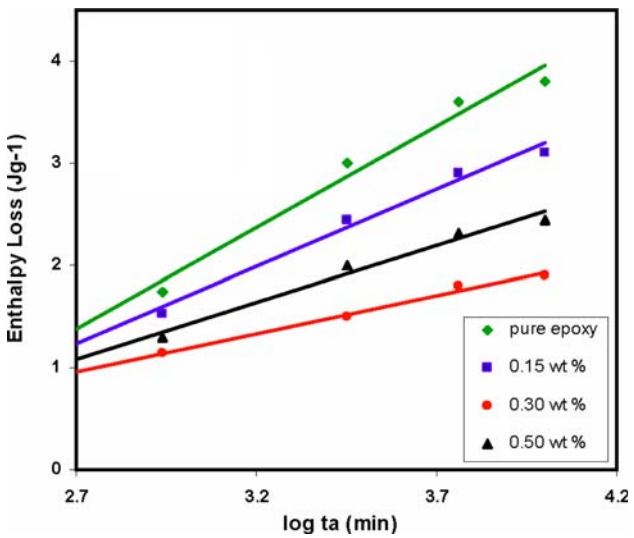

Fig. 8 Enthalpy loss as a function of logarithmic annealing time

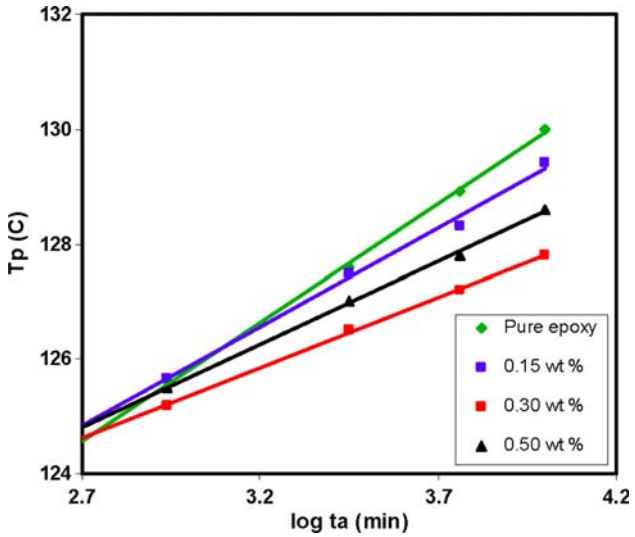

Fig. 9 Endothermic peak temperature as a function of logarithmic annealing time

$$S(q_1) = \left(\frac{\partial T_p}{\partial \ln|q_1|}\right)_{\delta_H, q_2} \tag{4}$$

$$S(\delta_H) = \left(\frac{\partial T_p}{\partial \delta_H}\right)_{q_1, q_2} \tag{5}$$

$$S(q_2) = \left(\frac{\partial T_p}{\partial \ln|q_2|}\right)_{\delta_H, q_1} \tag{6}$$

where q_1 is the cooling rate from equilibrium above T_g to annealing temperature, δ_H enthalpy loss at annealing temperature and q_2 reheating rate until equilibrium condition above T_g.

These shifts can be normalized by defining dimensionless variables $Q_1 = \theta q_1$, $D = \theta \delta_H/\Delta C_p$, $Q2 = \theta q_2$, and $T_1 = \theta T_p$ giving normalized shifts as [20]:

$$S(Q_1) = \theta\left(\frac{\partial T_p}{\partial \ln|q_1|}\right)_{\delta_H, q_2} \tag{7}$$

$$S(D_H) = \Delta C_p\left(\frac{\partial T_p}{\partial \delta_H}\right)_{q_1, q_2} \tag{8}$$

$$S(Q_2) = \theta\left(\frac{\partial T_p}{\partial \ln|q_2|}\right)_{\delta_H, q_1} \tag{9}$$

where θ is a temperature factor related to apparent activation energy:

$$\theta \approx \frac{\Delta h*}{RT_g^2} \tag{10}$$

It was shown that the shifts are all inter-related and $F(\chi)$ can be obtained from the master curve of $F(\chi)$ versus χ [21]:

$$F(\chi) = S(D_H) = S(Q_2) - 1 = -S(Q_1) \tag{11}$$

To evaluate χ from master curve, we used Eq. (11) with $F(\chi) = S(D_H)$. The values of ΔC_p are listed in Table 2 for different concentrations of r-GNFs in epoxy network.

Figure 10 displays the non-linearity parameter, χ, as a function of r-GNF wt% for the nano-epoxy systems. It revealed that the increase of r-GNF concentration up to 0.3 wt%, χ, decreased from 0.56 ± 0.03 to 0.46 ± 0.01. The similar results were obtained by Lu and Nutt [18] for the nano-clay/epoxy nano-composites. However, the variation of non-linearity with clay contents for their system was relatively smaller (χ: 0.30–0.26 for 0–10 phr of nano-clay) compared to the values achieved in our research work shown in Fig. 10.

According to a published report [22], the local structure of epoxy network is the most governing parameter for the non-linearity during enthalpy relaxation and the effect of supermolecular structure is negligible. In intercalated nano-composite systems, incorporating clay into the epoxy network makes a physical change in the local structure of epoxy network. However, in the present nano-epoxy system, the reactive hydrogen in the –OH– group can cause nanofibers to become involved in the curing reaction among epoxy networks, and then the nanofibers become incorporated into the cured epoxy structures. This leads to the change in the local chemical structure of epoxy network in which r-GNFs can restrict more areas of epoxy network around the r-GNFs through the chemical bonding between r-GNFs and epoxy resin. Thus, the restriction effect or confinement function is stronger, which led to lower non-linearity parameter values (stronger non-linearity) for nano-epoxy system over the neat epoxy resin. The facts that higher concentration of r-GNFs did not lead to smaller non-linearity, and the lowest non-linearity parameter χ appeared for the nano-epoxy with 0.3 wt% of r-GNFs, indicates that the restriction effect by the nanofibers plays an important role through appropriate amount of diluent in the system.

It can be concluded that in the present system, both physical and chemical changes in the local structure of epoxy network affect the non-linearity parameter. These results also imply that to reduce the contribution of temperature in the relaxation processes (aging during service caused by temperature) of an epoxy resin, adoption of an optimum amount of reactive nano-materials forming an improved bonding with epoxy network is more effective than using nano-materials which are only intercalated in epoxy network.

Table 2 ΔC_p values for r-GNFs/epoxy

ΔC_p	r-GNFs wt%
0.225	0
0.213	0.15
0.159	0.30
0.179	0.50

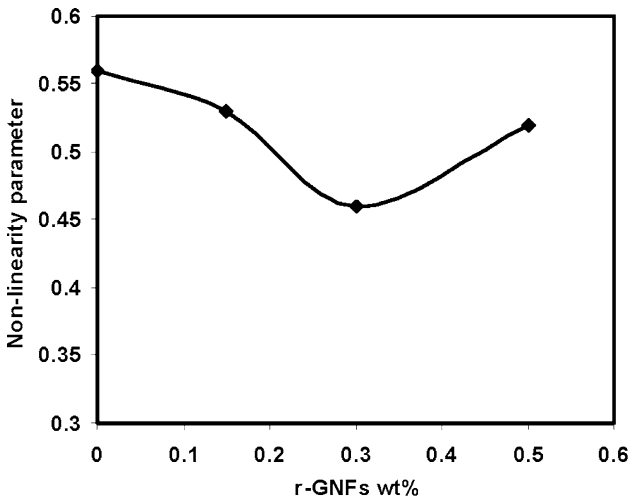

Fig. 10 Non-linearity parameter as a function of r-GNFs wt%

Non-exponentiality, β

Enthalpy experiments by DSC allow the evaluation of non-exponentiality parameter, β, either by curve fitting [23], or by measuring the height of the endothermic peak as a function of the prior cooling rate [10]. However, it has been shown that MDSC can provide a convenient method to obtain the non-exponentiality parameter [24]. Montserrat and Hutchinson introduced a method to determine β based on calorimetric measurements by MDSC [24]. They showed that the inflectional slope of the complex heat capacity, C_p* depends strongly on the exponential parameter of the Kohlrausch–William–Watts equation, which is inversely related to the β. They defined non-exponentially parameter as a normalized slope of complex heat capacity at T_g as follow:

$$\beta = 0.035 + 2.782(S/\theta) \tag{12}$$

where, S is the inflectional slope of C_p*,$S = ((dC_p*/dT)/\Delta C_p*)$, and $\theta = \Delta h*/RT_g^2$.

To apply this approach, the normalized dimensionless slope of S/θ can be evaluated from the C_p* signal of MDSC [24]. The values of S and S/θ for each specimen are listed in Table 3. These values agree very well with the range of values reported for epoxy specimens by Montserrat and Hutchinson [24]. Inserting these values in Eq. (12), the non-exponentiality parameter β of specimens with different concentrations of r-GNFs has been obtained.

From Fig. 11, it can be seen that β was decreased from 0.30 ± 0.01 for pure epoxy to 0.23 ± 0.03 for epoxy resin with 0.3 wt% of r-GNFs. This result is comparable to values obtained by Lu and Nutt [18] on nano-clay/epoxy composites. The decrease in β values with increasing r-GNFs (up to 0.3 wt%) implies a broadened distribution of relaxation time.

It has been shown that the non-exponentiality parameter β is independent of diluent effect [25]. Therefore, It is reasonable to consider that the change in β is caused by the restriction effect of the r-GNFs in our nano-epoxy system. As discussed above, r-GNFs can restrict more areas of epoxy network around the r-GNFs through the chemical bonding between r-GNFs and epoxy resin. Thus, the restriction effect or confinement function is stronger for the segments in the network near the nanofibers. Contrary to the coarse-grained domain relaxation model for the intercalated polymer nano-composite system [18], we proposed a continuous radiation model for our nano-epoxy system, which is a thicker (larger) interphase layer (zone) around a nanofiber with continuous and gradual reduction in restriction effect with increasing distance of the nanofiber to segments. In this model, the nanofibers are located in the middle, and the interphase zone around the nanofibers is composed of segments with gradually reduced restriction of the relaxation. The closer the segments are to the nanofibers, the slower relaxation those segments display, and thus form a radiation configuration in terms of the mobilization of segments. With increasing r-GNF content, more segments are immobilized on the nanofibers surface through the covalent bonding between r-GNFs and epoxy resin. At he same time, more r-GNFs result in shorter distance among nanofibers, and consequently, fewer segments with the faster segmental motions. Therefore, contributions from both faster and slower segmental motions increase and finally give rise to the observed decrease in β values at the intermediate level of r-GNFs such as 0.3 wt%. These results suggest that the epoxy network with optimum amount of r-GNFs (0.3 wt%) shows the most resistance of the nanofibers in local environment to structural changes, and consequently the smallest dimensional change from rubbery state to glassy state.

Table 3 T_g and inflectional slope of complex heat capacity for r-GNFs/epoxy

r-GNFs wt%	T_g (°C)	S (K^{-1})	Θ (K^{-1})	S/θ
0	133.0	0.052	0.539	0.097
0.15	135.5	0.060	0.743	0.081
0.30	137.5	0.061	0.848	0.071
0.50	136.6	0.054	0.691	0.079

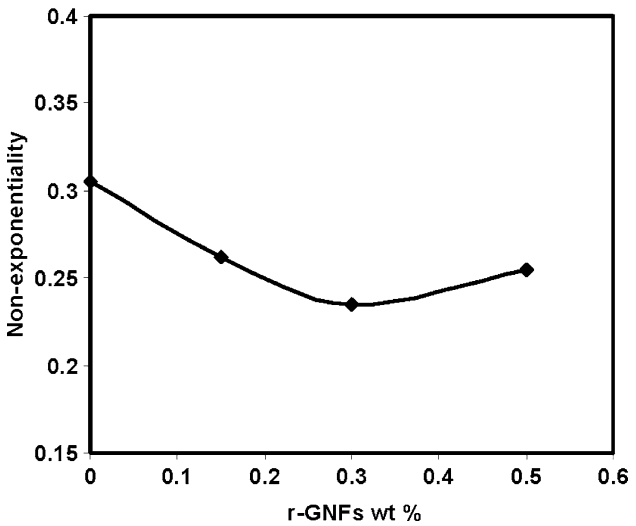

Fig. 11 Non-exponentiality parameter as a function of r-GNFs wt%

Conclusions

The relaxation phenomena of an epoxy resin modified by different concentrations of r-GNFs (up to 0.5 wt%) has been investigated by standard and modulated DSC. Results showed that incorporation of r-GNFs into the epoxy crosslink network (even at low concentrations of r-GNFs) have a significant effect on the segmental relaxation of the resin system. The nano-epoxy exhibited slower relaxation dynamics, higher apparent activation energy (higher value of Δh^*), greater non-linearity (lower value of χ), and broader relaxation time distribution (lower value of β) than the neat epoxy resin. These values were optimum for the three values evaluated for the nano-epoxy with 0.3 wt% of r-GNFs, which indicated the nano-epoxy with this concentration of r-GNFs would have the best dimensional stability during service. This study is in agreement with the expectation on small values of χ correlating with small values of β and large Δh^*.

Acknowledgements The authors gratefully acknowledge the support from NASA through Grant NNM04AA62G. We also gratefully acknowledge Dr. Charles M. Lukehart and Mr. Jiang Li (Vanderbilt University) for providing the functionalized graphitic nanofibers.

References

1. Liu Y, Zheng S, Nie K (2005) Polymer 46:12016
2. Wingert MT (2004) Master thesis, Improvement of interfacial adhesion between UHMWPE fiber and Epoxy matrix using graphitic carbon nanofiber, North Dakota State University, Fargo, ND
3. Chiang MYM, Mckenna GB, Yuan J (1994) Polym Eng Sci 34:1815
4. Blair C, Zakrzewski J (1991) SAMPE Q 22(3):2
5. Hwang JJ, Liu HJ (2001) Macromolecules 34:8686
6. Liu HJ, Hwang JJ, Chen-Yang YW (2002) J Polym Sci Part A: Polym Chem 40:3873
7. Dubief D, Samain E, Dufresne A (1999) Macromolecules 32:5765
8. Bessel CA, Laubernds K, Rodriguez NM, Baker RTK (2001) J Phys Chem 105:1115
9. Li J, Vergne MJ, Mowles ED, Zhong WH, Hercules DM, Lukehart CM (2005) Carbon 43:2883
10. Hutchinson JM, Ruddy M (1991) J Polym Sci Polym Phys 28:2127
11. van der Linde R, Belder EG, Perera DY (2000) Progr Org Coatings 40:215
12. Tool AQ (1946) J Am Ceram Soc 29:240
13. Narayanaswamy OS (1971) J Am Ceram Soc 54:491
14. Moynihan CT, Easteal AJ, De Bolt MA, Tucker J (1976) J Am Ceram Soc 59:12
15. Ramirez C, Abad MJ, Cano J, Lopez J (2001) Colloid Polym Sci 279:184
16. Williams G, Watts DC (1970) Trans Faraday Soc 66:80
17. Woo EM, Kuo SM (1997) Polym Eng Sci 37:173
18. Lu H, Nutt S (2003) Macromol Chem Phys 204:1832
19. Zhong WH, Li J, Xu LR, Lukehart CM (2005) Polym Comp 26:128
20. Hutchinson JM, Kumar P (2002) Thermochim Acta 391:197
21. Zheng Y, Simon SL, Mckenna B (2002) J Polym Sci Part B: Polym Phys 40:2027
22. Calventus Y, Montserrat S, Hutchinson JM (2001) Polymer 42:7081
23. Hodge IM (1994) J Noncryst Solids 169:211
24. Montserrat S, Hutchinson JM (2002) Polymer 23:351
25. Cortes P, Montserrat S, Hutchinson JM (1997) J Appl Polym Sci 63:17